SEMARAK ILMU PUBLISHING

Journal of Advanced Research in Numerical Heat Transfer

Journal homepage:
https://semarakilmu.com.my/journals/index.php/arnht/index
ISSN: 2735-0142

Lattice Boltzmann Computation of Steady Cross-Flow Across a Rectangular Obstacle with Different Aspect Ratio: Effect of Blockage Ratio

Krunal M. Gangawane[1,*]

[1] Department of Chemical Engineering, National Institute of Technology Rourkela, Rourkela - 769008, Odisha, India

ARTICLE INFO

Article history:
Received 7 March 2023
Received in revised form 13 April 2023
Accepted 15 May 2023
Available online 30 June 2023

Keywords:
Rectangular cylinder; Lattice Boltzmann Method; Blockage ratio; Aspect ratio; Reynolds number; Drag coefficient

ABSTRACT

This work presents a two dimensional lattice Boltzmann analysis of steady and cross-flow of Newtonian fluid across a built-in rectangular cylinder. In particular, the effects of the blockage ratio andaspect ratio of rectangular cylinder (width/height) on the momentum characteristics have been explored for range of flow governing parameters such as, blockage ratio (β = 1/8, 1/12, 1/16), aspectratio of rectangular cylinder ($1 \leq a_r \leq 6$) at constant Reynolds number of *Re* = 40 correspondingto the laminar range. The physical insight of system is gained by evaluation of stream-function, vorticity and pressure coefficient variation, etc. Further, the engineering gross parameter, such as drag coefficient is determined for possible use in engineering design purpose. It is observed that the increase in blockage ratio drag coefficient values decreases and drag values show proportional variation with aspect ratio. Finally, a closure relationship is developed between drag coefficient, blockage ratio and aspect ratio of rectangular cylinder for possible use in engineering/scientific practices.

1. Introduction

A considerable amount of research work has been devoted well over past few decades to investigate the flow past heated obstacles of varying shapes (viz., circular, square, triangular) owing to its wide range of applications in industrial and domestic fields. Additionally, this problem is considered as classical fluid flow problem in the field of transport phenomenon, as it exhibits variety of fluid flow characteristics. The bulk of literature referring to cylinder of circular cross section followed by square, elliptical and rectangular is available. The study of flow past a square/rectangular cylinder is very important for knowledge of engineering physical parameters such as drag coefficient, Nusselt number, wake size, etc., which are often used for the design of cooling towers, antennas, chimneys, antennas, support structures, high rise building etc [1-3]. It is clearly evident that, the wall confinement has remarkable influence on the detailed kinematics of flow field. Therefore, the fluid nature and asperity of blockage may either intensify or impede the drag on rectangular cylinder [4]. As far as known to us, there has been no prior work on effect of higher blockage ratio on fluid flow

* *Corresponding author.*
E-mail address: krunalgangawane@gmail.com (Krunal M. Gangawane)

https://doi.org/10.37934/arnht.13.1.117

behavior of built-in rectangular cylinder by using lattice Boltzmann method (LBM) which constitutes the main objective of the present work. The present work aims to elucidate the influence of blockage ratio (wall confinement) and aspect ratio of rectangular cylinder on laminar, steady state, fluid flow characteristics in a flow past a rectangular cylinder by using lattice Boltzmann method (LBM). Before presenting the new results obtained in current study, it is always utile to recollect the scant literature on steady flow past a built in rectangular cylinder.

2. Previous Work

There is voluminous literature now available for flow past a circular and square cylinder for laminar as well as turbulent condition and blockage ratios. However, very few studies have been illustrated the fluid flow characteristics of steady cross flow past a rectangular cylinder for combined effect of aspect ratio of rectangular cylinder and blockage ratio. For instance, Okajima [5] experimentally investigated the vortex-shedding frequencies of various rectangular cylinders in a wind tunnel and in a water tank. The aspect ratio of rectangular cylinder in their study was a = 2 and 3 for range of Reynolds number ($70 \leq Re \leq 2 \times 10^4$). The critical Reynolds number shown strong dependence upon the aspect ratio of the cylinder in their study. Similarly, Davis and Moore [6] and Davis *et al.,* [7] numerically analyzed the vortex shedding from rectangular cylinder in unconfined and confined channel domain, respectively. The flow governing parameters used in their study was Reynolds number ($100 \leq Re \leq 280$), blockage ratio (1/4, 1/6), aspect ratio ($1 \leq a_r \leq 4$) and ($0.6 \leq a_r \leq 1.7$) and upstream velocity profile. They observed increase in drag and Strouhal number with increase in channel confinement (decrease in blockage ratio). Subsequently, Norberg [8] presented the experimental study of flow around rectangular cylinders to investigate the pressure forces and wake frequencies for range of flow governing parameters (aspect ratio: $1 \leq a \leq 3$, Reynolds number: $4 \leq Re \leq 3 \times 10^4$, angle of attack of cylinder: $0^o - 90^o$). They observed multiple wake frequencies at small angles of attack for certain range of Reynolds number and with aspect ratio = 2-3. Later, the numerical investigation of unsteady flow-Reynolds number (≤ 200) flow around rectangular cylinder with aspect ratio ($1 \leq a_r \leq 4$) at angle of incidence ($0^o - 90^o$) is reported by Sohankar *et al.,* [9]. The flow separation at downstream corners is observed for cases with one side opposing flow at Re = 100. Yang and Fu [10] reported the fluid flow and heat transfer characteristics from an oscillating rectangular cylinder for wide range physical parameters such as, Reynolds number (Re = 250, 500), oscillating speed (0.333, 0.5, 1), oscillating amplitude (0.125, 0.333, 0.5, 0.75), aspect ratio (a = 1, 2) and blockage ratio (β = 0.1, 0.2). They observed heat transfer enhancement with aspect ratio of rectangular cylinder.

Nitin and Chhabra [11] elucidated the combined effect of non-Newtonian power law index ($0.5 \leq n \leq 1.4$), Reynolds number ($5 \leq Re \leq 40$), Peclet number ($5 \leq Pe \leq 400$) and blockage ratio (β = 1/8) on momentum and heat transfer characteristics from heated built-in rectangular cylinder of aspect ratio (width/height) of 2. They observed increase in power law index caused decrease in both drag and Nusselt number values. A three dimensional numerical study of turbulent, separated and reattached flow around rectangular cylinder is reported by Bruno *et al.,* [12].

Subsequently, the lattice Boltzmann simulation of flow past a rectangular cylinder with different aspect ratio have been reported by Islam *et al.,* [13]. The aspect ratio of rectangular cylinder used in their study are $0.15 \leq a \leq 4$ for Reynolds number of Re = 100, 150, 200, 250 and a constant blockage ratio of β = 1/12. They observed discontinuity in the range of $1.25 \leq a_r \leq 1.6$, obtained from multiple peaks by Fourier spectrum analysis of the lift force.

Recently, Chen and Shao [14] delineated experimentally the vortex shedding suppression from a rectangular cylinder. The physical parameters used in their study was Reynolds number (Re = 75 −

130) for constant aspect ratio of rectangular cylinder a_r = 3. They observed the effective zone of square element reduces with increasing Reynolds number and disappears at *Re* > 130.

Thus, the brief review of literature suggests that there is very little information elucidating the influence of the aspect ratio of rectangular cylinder and blockage ratio on momentum characteristics. Most of the studies have investigated the effect of wall confinement for a narrow range (≤ 1/8). None of the study, as much known to us, have studied higher blockage ratio (or less wall confinement) effect on momentum characteristics. The present study aims to fill the gap found in literature. In particular, field equations are solved by using lattice Boltzmann method for wide range of aspect ratio and blockage ratio at constant Reynolds number of Re = 40 to get the detailed flow fields around the rectangular cylinder. It is further used for evaluating the gross engineering parameters such as drag coefficients, pressure coefficients, local and average Nusselt number. The blockage ratio is varied in the step of 1/4 as 1/8, 1/12, 1/16 and constant Reynolds number *Re* = 40. The description of Problem, mathematical formulation and numerical methodology used for present problem are discussed in proceeding sections.

3. Problem Definition and Mathematical Formulation

Consider a two dimensional, steady, laminar flow of incompressible Newtonian fluid across a built-in rectangular cylinder with uniform velocity (U_∞) confined in a channel of height *H* and length *L*. The blockage ratio is defined as the ratio of size of cylinder wall to the height of channel wall ($\beta = \frac{b}{H}$). The aspect ratio (a_r) of rectangular cylinder is defined by a_r = *b/w*, where, 'b' is height and 'w' is width of rectangular cylinder (as shown in Figure 1). The rectangular cylinder is placed at a sufficient distance from inlet (L_u = 10), such that it remains free from entrance effects.

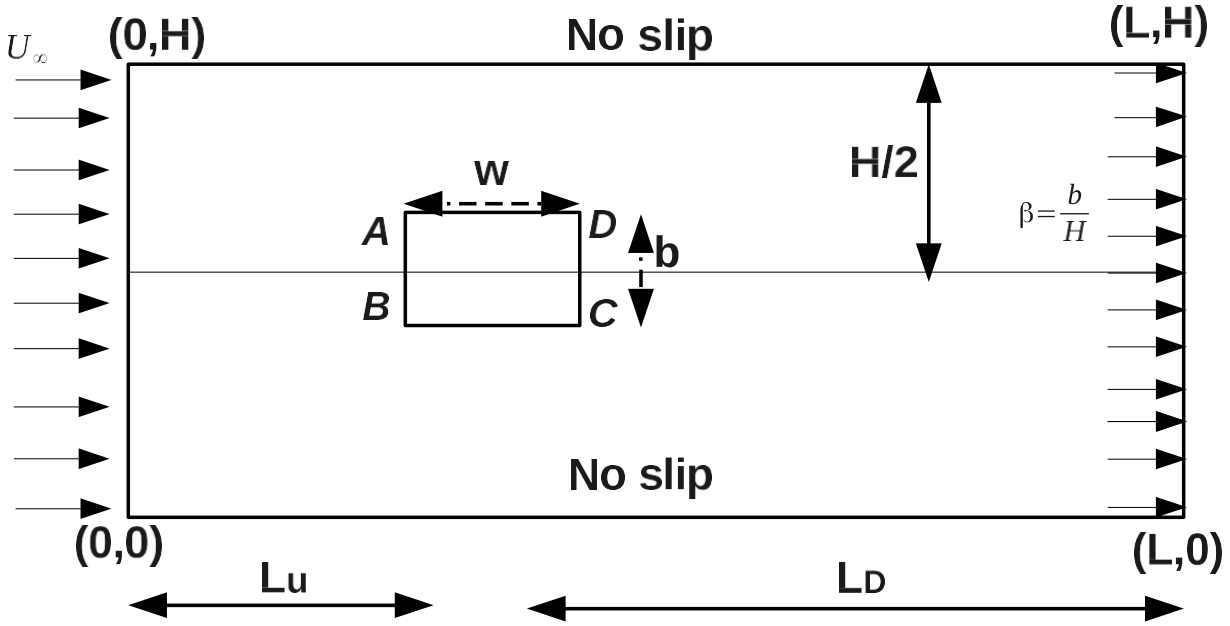

Fig. 1. Schematic representation of confined flow past a rectagular cylinder (physical as well as computational domain)

Under the above-noted simplified assumptions, the flow governing equations of steady cross-flow of Newtonian fluid, namely, mass and momentum in non-dimensional form are expressed as follow:

$$\frac{\partial U_x}{\partial X} + \frac{\partial U_y}{\partial Y} = 0 \tag{1}$$

$$\left(U_x \frac{\partial U_x}{\partial X} + U_y \frac{\partial U_x}{\partial Y}\right) = -\frac{\partial P}{\partial X} + \frac{1}{Re}\left(\frac{\partial^2 U_x}{\partial X^2} + \frac{\partial^2 U_x}{\partial Y^2}\right) \tag{2}$$

$$\left(U_x \frac{\partial U_y}{\partial X} + U_y \frac{\partial U_y}{\partial Y}\right) = -\frac{\partial P}{\partial Y} + \frac{1}{Re}\left(\frac{\partial^2 U_y}{\partial X^2} + \frac{\partial^2 U_y}{\partial Y^2}\right) \tag{3}$$

In Eq. (1) to Eq. (3), reference length (b), reference velocity (U_{avg}) and reference pressure ($\rho {U^2}_{avg}$) are used to scale the length, velocities and pressure, respectively. With the boundary conditions of the specified problem,

At inlet boundary ($X = 0$): Uniform flow

$$U_x = 1, U_y = 0 \tag{4}$$

At upper and lower boundary, ($Y = 0,1$): No Slip

$$U_x = 0, U_y = 0 \tag{5}$$

On the surface of rectangular cylinder: No slip

$$U_x = 0, U_y = 0 \tag{6}$$

At exit boundary: The homogeneous Neumann boundary condition

$$\frac{\partial \phi}{\partial X} = 0 \tag{7}$$

where $\phi = U_x, U_y$.

The dimensionless groups appearing in above equations are represented as follows:

Reynolds number

$$Re = \frac{bU_{avg}}{V} \tag{8}$$

Eq. (1), Eq. (2), and Eq. (3) along with above mentioned boundary conditions (Eq. (4) to Eq. (7)) are solved by using lattice Boltzmann solution procedure, for estimating detailed velocity and pressure fields, which in turn are used for obtaining engineering gross parameters such as drag coefficients, stream function, pressure coefficients, etc. The mathematical expressions of such engineering gross parameters are described below:

The drag coefficient in non-dimensional form is represented as below [15,16]:

$$C_D = \frac{F_D}{0.5\rho {U^2}_{avg} b} \tag{9}$$

where, FD is drag force exerted on square cylinder per unit length. C_D is normal force component (in z direction). While, x and y components are friction drag (C_{DF}) and pressure drag (C_{DP}), respectively. The pressure or form drag component is estimated by integrating pressure on two vertical faces of square cylinder. It is expressed as,

Pressure drag coefficient

$$C_{DP} = 2\left(\int_A^B PdY - \int_C^D PdY\right) \tag{10}$$

In similar manner, the friction drag coefficient along top and bottom walls of square cylinder can be evaluated as,

$$C_{DF} = \frac{2}{Re}\int\left(\frac{\partial U_x}{\partial Y}\right) \tag{11}$$

The total drag coefficient is calculated as,

$$C_D = C_{DP} + C_{DF} \tag{12}$$

The one of the advantages of LBM lies in the fact that unlike conventional CFD tools, estimation of the pressure field is very easy. For uniform lattice size it is given as below [17],

$$P = c_s^2\rho = \frac{1}{3}\rho; \qquad \text{where } \left(c_s = \frac{1}{\sqrt{3}}\right) \tag{13}$$

Surface pressure coefficient (C_P), it is defined as ratio of static pressure on the surface of square cylinder to that of free stream pressure [18]. It is expressed as follows:

$$C = 2\left(\frac{P_S - P_\infty}{\rho {U^2}_{avg}}\right) \tag{14}$$

where P_S is pressure at the surface of square cylinder and P_∞ corresponds to free stream pressure.

The flow governing differential equations (viz., mass and momentum) have been solved numerically by using a mesoscopic, numerical tool called lattice Boltzmann method (LBM). The lattice Boltzmann method (developed in C++ programming language) is used for solving field equations. The equations and methodology of lattice Boltzmann method is described in ensuing section.

4. Numerical Method: Lattice Boltzmann Method

In recent decennary, the lattice Boltzmann method (LBM) has been developed as a prominent computational/numerical tool for analyzing the complex fluid and heat transfer phenomenon. Among other computational methods, the development of LBM has been greatly appreciated recently in the fields of science and engineering as one of the potential computational fluid dynamic tools. It is particularly successful in fluid flow applications involving inter-facial dynamics, droplet dynamic, multi-phase, multi-component flows and complex boundaries [17,19-23].

The conventional computational tools such as, finite difference method, finite element method and finite volume method, etc, are based on discretization of macroscopic continuum equations

whereas mesoscopic lattice Boltzmann method (LBM) is based on microscopic models and mesoscopic kinetic equation (Boltzmann equation). In LBM, the simplified kinetic models are formed, such that it includes the essential physics of microscopic or mesoscopic processes and microscopic averaged properties are suitable delineation of the desired macroscopic field equations. The advantages of kinetic nature of LBM over conventional CFD method are simplicity in understanding and coding, implementation of boundary conditions at leisure due to use of particle distribution functions rather than macroscopic variables, ease of parallel computing and handling of complex geometries. In conventional computational fluid dynamics (CFD) methods, estimation of pressure field is normally time consuming as one has to solve Poisson like equation derived from incompressible Navier-Stokes equation, whereas pressure field calculation is extremely simple in LBM as it is done by simply using equation of state. Furthermore, convection operator is linear, and by simple arithmetic calculations, microscopic distribution functions can be transferred to macroscopic physical quantities [17,24].

A time integration of the Boltzmann equation in any direction 'kJ results in the basic lattice Boltzmann equation (LBE). The flow field lattice Boltzmann equation are expressed as below:

$$f_k(x + e_k\Delta t, t + \Delta t) - f_k(x,t) = -\frac{1}{T_v}\left[f_k(x,t) - f_k^{eq}(x,t)\right] \tag{15}$$

The equilibrium distribution function (f_k^{eq}) is expressed as follow:

$$f_k^{eq}(x,t) = \rho w_k\left[1 + \frac{3(u\cdot e_k)}{c^2} + \frac{9(u\cdot e_k)^2}{2c^4} + \frac{3(u\cdot u)}{2c^2}\right] \tag{16}$$

where, τ_v, f_k^{eq}, g_k^{eq}, Δt, $\Delta x(e_k\Delta t)$ and $c\left(\frac{\Delta x}{\Delta t} = 1.0\right)$ are relaxation parameter, equilibrium distribution function, lattice time step, lattice space step and lattice streaming speed, respectively. u is velocity vector, e_k is lattice link direction. For *D*2*Q*9 lattice model (two dimensional, nine velocity link model), w_k is equilibrium distribution of weight for direction k, is given as,

$$w_k = \begin{cases} \frac{4}{9} & k = 0 \\ \frac{1}{9} & k = 1,2,3,4 \\ \frac{1}{36} & k = 5,6,7,8 \end{cases} \tag{17}$$

The discrete velocity links for *D*2*Q*9 lattice model are expressed as,

$$e_0 = (0,0) \tag{18}$$

$$e_1 = (1,0); \quad e_2 = (0,1) \quad e_3 = (-1,0) \quad e_4 = (0,0) \tag{19}$$

$$e_5 = (1,1); \quad e_6 = (-1,1) \quad e_7 = (-1,-1) \quad e_8 = (1,-1) \tag{20}$$

The flow field relaxation time (τ_v) are related to kinematic viscosity (v), for *D*2*Q*9 model, and are represented as follows [17,24,25]:

$$\tau_v = 3.0v + \frac{1}{2} \tag{21}$$

The macroscopic quantities such as density and velocity fields are calculated as,

$$\rho = \sum_k f_k \tag{22}$$

$$\rho u = \sum_k f_k e_k \tag{23}$$

By Champman-Enskog analysis, it has been proved that mass and momentum equations can be recovered up to second order from Eq. (15), respectively [17].

4.1 Implementation of Boundary Conditions

The proper and accurate implementation of boundary conditions is considered as an important step for all the numerical solvers. In LBM boundary conditions are designated by unknown particle distribution function directing from boundary wall towards flow field. For no slip walls, bounce back method of non-equilibrium distribution function developed by Zou and He [26] is used. In bounce back condition, particle distribution functions after solid wall nodes move back to node it has come from with same lattice link direction bounces back to the original position. For flow field, unknown distribution functions at no-slip boundary of domain are estimated by following equations:
No slip wall: Bounce back condition,

$$f_k - f_k^{eq} = f_k - f_k^{eq} \tag{24}$$

At west wall or inlet (*X = 0*), velocity is assigned. For such cases, von Neumann flux boundary condition as proposed by Zou and He [26] is useful. It is represented as given below:

$$\rho_0 = \frac{f_0+f_2+f_4+2(f_3+f_6+f_7)}{1-u_0} \tag{25}$$

$$f_1 = f_3 + \frac{2}{3}\rho_0 u_0 \tag{26}$$

$$f_5 = f_7 + \frac{1}{2}(f_2 - f_4) + \frac{1}{6}\rho_0 u_0 \tag{27}$$

$$f_8 = f_6 + \frac{1}{2}(f_2 - f_4) + \frac{1}{6}\rho_0 u_0 \tag{28}$$

For outlet boundary (*X = 1*), extrapolation scheme of Mohamad [25] is used for estimating unknown distribution functions. It is expressed as below:

$$f_3 = 2f_{3,nx-1} - f_{3,nx-2}; \quad f_6 = 2f_{6,nx-1} - f_{6,nx-2}; \quad f_7 = 2f_{7,nx-1} - f_{7,nx-2} \tag{29}$$

where, ρ_0, u_0 and nx are density and velocity at inlet wall (*X = 0*), lattice node on east/outlet wall (*X = 1*), respectively.

4.2 Numerical Algorithm

The algorithm of lattice Boltzmann method solver (developed in C++ programming language) is described below:

(i) Initialization of domain with initial density ($\rho > 0$) and velocity ($U_x = 0, U_y = 0$).
(ii) Determination of flow field followed by following steps,
    (a) Collision step.
    (b) Streaming.
    (c) Boundary conditions.
    (d) Estimation of macroscopic quantities (density and velocity).
(iii) Check for the convergence.
    (a) If converged, evaluate step 4.
    (b) Else repeat step 2 to 3.
(iv) Process the flow and thermal fields to estimate the local and global variables.

The numerical simulations are carried out until the following convergence criterion is fulfilled. For convergence of solution absolute error criterion is used for velocity and temperature fields. It is represented as follows,

$$\in = max|\phi_{new} - \phi_{old}| \leq 10^{-8} \tag{30}$$

where, ϕ represents physical variables checked for convergence. In this study, these are velocity components u and v.

5. Numerical Parameters Choice

It is very well known that computational parameters (such as mesh and domain sizes) have significant influence on the reliability and accuracy of the numerical simulation results. Therefore, proper choice of the numerical parameters, namely, the upstream and downstream lengths and grid size is foremost before presenting the new results. In present work, the height of rectangular cylinder (*b*) is used for characterizing the domain size. The choice of grid size and effect of upstream length are addressed in this section.

5.1 Grid Independence Study

In order to ensure the accuracy and reliability of present code, the grid independence study is carried out based on drag coefficient of rectangular cylinder. In this study, the adequacy of five uniform lattice sizes (grids) on height of rectangular cylinder, (G1 : 15, G2 : 16, G3 : 17, G4 : 20, G5 : 25) have been examined (as shown in Table 1). It is observed that relative error between coarsest grid (G1 : 15) with respect to finest grid (G5 : 25) is around 3.6%. The results shown insignificant changes from grid size G4 : 20 onward with the enormous increase in computational time to get converged solution. Therefore, 20 lattice nodes on height of cylinder, which is found to be optimum with respect to computational time and mesh size, is chosen in this study, which is believed to be sufficiently refine enough to resolve flow hydrodynamic features within interested range of conditions. The number of lattices along the width of rectangular cylinder are increased according to the aspect ratio.

Table 1
Grid independence study based on the height of rectangular cylinder (b) on drag coefficient (C_D) for Re = 40 and β = 1/8 for two aspect ratios (a = 1, 2)

	Number of lattice nodes				
a	$G1: 15$	$G2: 16$	$G3: 18$	$G4: 20$	$G5: 25$
1	1.752	1.738	1.715	1.699	1.692
2	1.934	1.915	1.868	1.856	1.851

5.2 Domain Independence Study

The proper choice of upstream and downstream length is very important in order to the keep numerical results free from entrance and exit effects. In this section, the effects of upstream and downstream length on flow field have been investigated.

A detailed examination of choice of upstream length on pressure and viscous drag coefficients have been done. The adequacy of four upstream lengths (L_u = 8, 10, 12, 14) at Reynolds number of Re = 40, aspect ratio of a = 6 and β = 1/8 have been investigated as shown in Figure 2. It can be observed that the changes are insignificant in the values of C_{DP}, C_{DF} and C_D for considered upstream length values. The percent changes in C_{DP}, C_{DF} and C_D in upstream lengths of 8 to that of 14 is observed to be 4.5%, 0.7% and 3.5%, respectively. Hence, in present work, upstream length of L_u = 10 is used, which can be considered as sufficient enough to keep results free from entrance effects. An additional numerical experiment has been conducted to investigate the effect of uniform velocity profile at inlet. It is observed that at L_u = 10, insignificant changes are observed in the estimated values of C_D. The total length of channel is assumed sufficiently large enough (L = 50) so that it does not affect flow characteristics near rectangular cylinder. Hence, the downstream length, L_d = 39, which is much higher than previous studies is used for all considered range of conditions [15,27]. The numerical parameters used in present study are: Upstream length, L_u = 10, downstream length L_d = 39, channel length, $L = L_u + b + L_d = 50$, the lattice size for domain, 1000 × 20(1/β). Thus, for β = 1/8, 1/12 and 1/16, the lattice size of domain become 1000 × 160, 1000 × 240 and 1000 × 320, respectively. For present numerical simulation a uniform lattice size is chosen, which is believed to be refine enough to resolve the thermal and flow phenomenon within interested range of conditions.

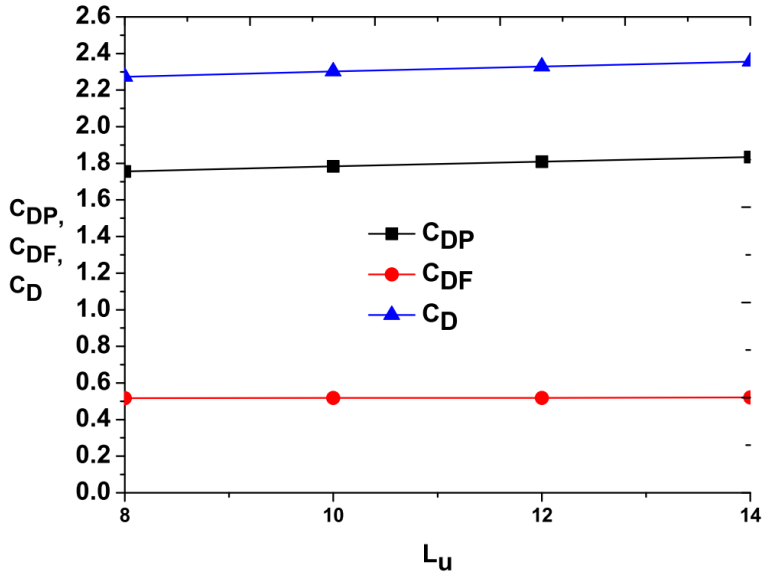

Fig. 2. Effect of upstream length (L_u) on pressure (C_{DP}), viscous (C_{DF}) and total drag (C_D) at Re = 40, β = 1/8 and aspect ratio (a) = 6

6. Results and Discussions

In this study, the lattice Boltzmann method (LBM) solver based on D2Q9 lattice model (developed in C++ programming language) has been used to illustrate the steady state fluid flow characteristics from a built-in rectangular cylinder in channel flow. Extensive results have been obtained and presented herein this section for the following ranges of conditions.

(i) Reynolds number (*Re*): 40
(ii) Blockage ratio (β): 1/8, 1/12 and 1/16.
(iii) aspect ratio of rectangular cylinder (a_r): 1, 2, 4 and 6.

For these broad ranges of flow governing parameters, the local and global convective flow characteristics such as the evolution of stream-functions; vorticity; Pressure and friction coefficient; and the drag coefficients are obtained and discussed herein the proceeding sections.

6.1 Validation of Results

The reliability and accuracy of present numerical simulation is examined by comparing the results obtained from present numerical procedure with previous reported studies. The validation is based on drag coefficient (C_D) values estimated along built-in square and rectangular cylinder (a = 2) for range of parameters considered herein. Table 2 presents comparison between results obtained from present simulation with previous studies of square cylinder and rectangular cylinder [11,16,27,28]. As can be seen from Table 2, present results show excellent agreement with literature. The minimum, maximum and average error of C_D between present results with that of literature are and 1.5% and 3.5%, respectively for square (aspect ratio, a = 1) and rectangular cylinder (aspect ratio, a = 2). The present numerical simulation results are reliable in the range of ±3 − 4%. Such a minor errors tend to arise due to the factors such as numerical method, grid size, convergence criterion, numerical errors (round up and programming) etc. Results presenting in this study are accurate and reliable in the range of 3 − 4%. With the above comparison between our developed code for channel flow across a built-in square/rectangular cylinder in channel with the literature data, it is sufficed to say that our results are quantified. This ascertains and inspires the confidence in accuracy and reliability of present in-house LBM solver. The effect of blockage ratio and aspect ratio of rectangular cylinder on fluid flow characteristics are discussed in next section.

Table 2
Comparison of drag coefficient (C_D) values at β = 1/8 and aspect ratio of a = 1, 2

Source	*Re* = 40
aspect ratio (a) = 1 (square)	
Present	1.699
Gupta *et al.,* [16]	1.871
Dhiman *et al.,* [27]	1.752
Bouaziz *et al.,* [28]	1.752
aspect ratio (a) = 2	
Present	1.726
Nitin and Chhabra [11]	1.921

6.2 Effect on Streamline and Vorticity Pattern

The local flow characteristics such as streamlines and vorticity profiles in the vicinity of the rectangular cylinder are analyzed herein to gain the physical insights into the nature of the hydrodynamics features of built-in rectangular cylinder in a plane channel. The influence of blockage ratio (β) on flow field in channel flow with built-in rectangular cylinder is delineated by evolution of streamlines, vorticity, drag coefficient, and pressure component variation along surface of rectangular cylinder for interested range of conditions. Figure 3 represents the stream-line patterns in the vicinity of square cylinder for interested range of blockage ratio (β) and Reynolds number (Re). The blockage ratio variation slightly affects stream-line patterns for a constant Reynolds number. It can be seen from Figure 3, at β = 1/8 for square cylinder (a = 1), the formation of re-circulation zone from the rear face of cylinder is observed [27]. The increase in β, has a very marginal increase in recirculation length. For a constant blockage ratio, the gradual increase in the aspect ratio of rectangular cylinder has significant influence on the physics of flow, as described by the decrease in the re-circulation length. The increase in distance between the front and rear face of cylinder (due to increase in aspect ratio), as anticipated, causes decrease in the wake region formation. Thus, the streamline patterns have a complex dependence on blockage ratio and aspect ratio of rectangular cylinder. The aspect ratio of rectangular cylinder has far more remarkable influence on streamline patterns than blockage ratio.

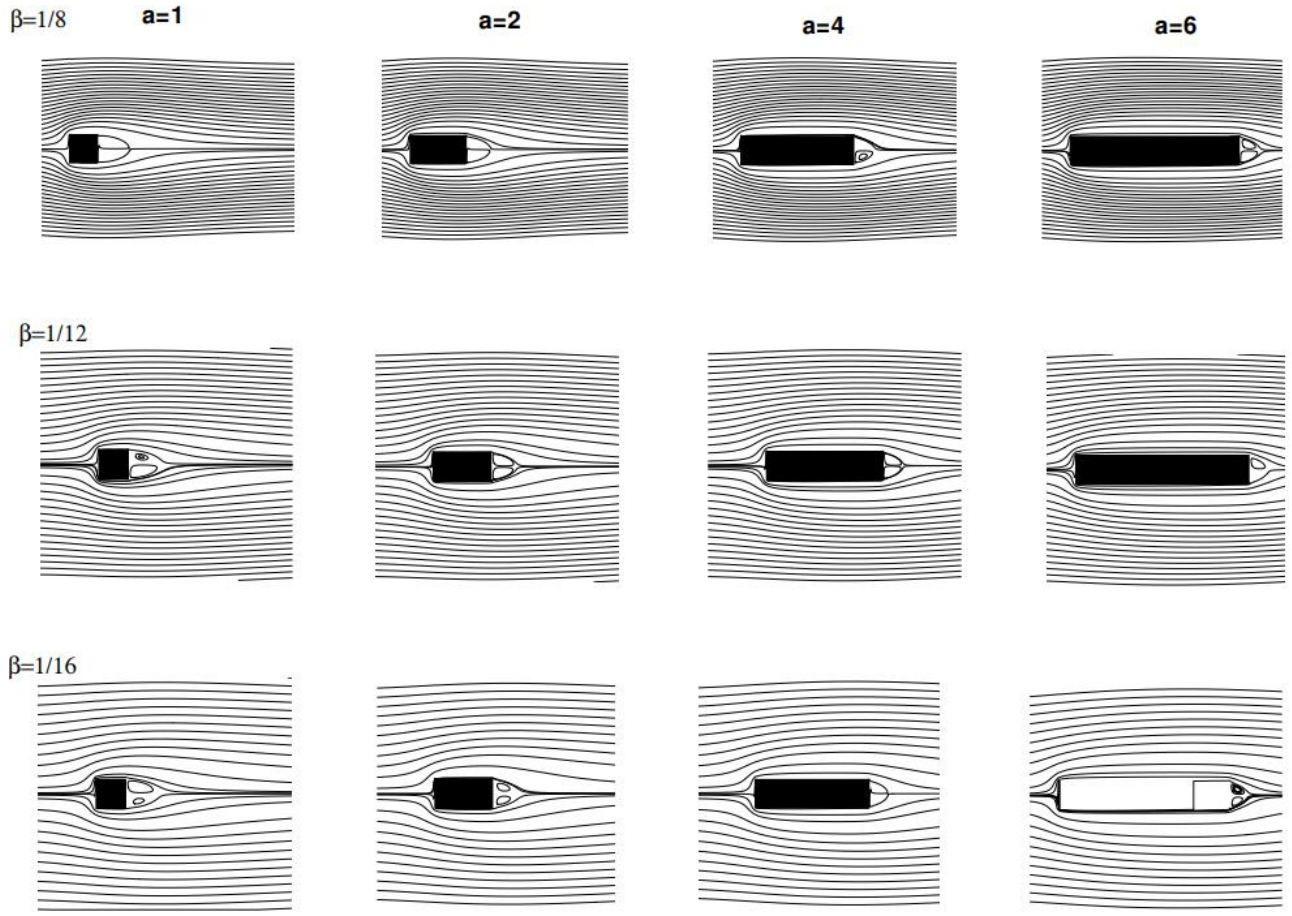

Fig. 3. Streamline patterns for different aspect ratio of rectangular cylinder (a = 1, 2, 3, 4) and blockage ratio (β = 1/8, 1/12.1/16) at Re = 40

The vorticity profile, as reported by Dhiman *et al.,* [15,27] and Bharti *et al.,* [29] are used for locating the separation points and fluid behavior near the surface of rectangular cylinder. Figure 4 shows the vorticity patterns for range of conditions considered herein. The increase in blockage ratio causes increase in the effective shearing [27]. For particular Reynolds number, the increasing in blockage ratio results in increase in vorticity magnitude with vorticity pattern remain nearly same. The increase in aspect ratio has substantial effect on the separation points near the rear face of rectangular cylinder. For a constant blockage ratio, with the increase in aspect ratio from a = 1 (square) to 2, 4, 6 causes the vorticity lines to become parallel to the longitudinal surface of rectangular cylinder. Thus, the aspect ratio of rectangular cylinder and blockage ratio slimly affects the vorticity patterns.

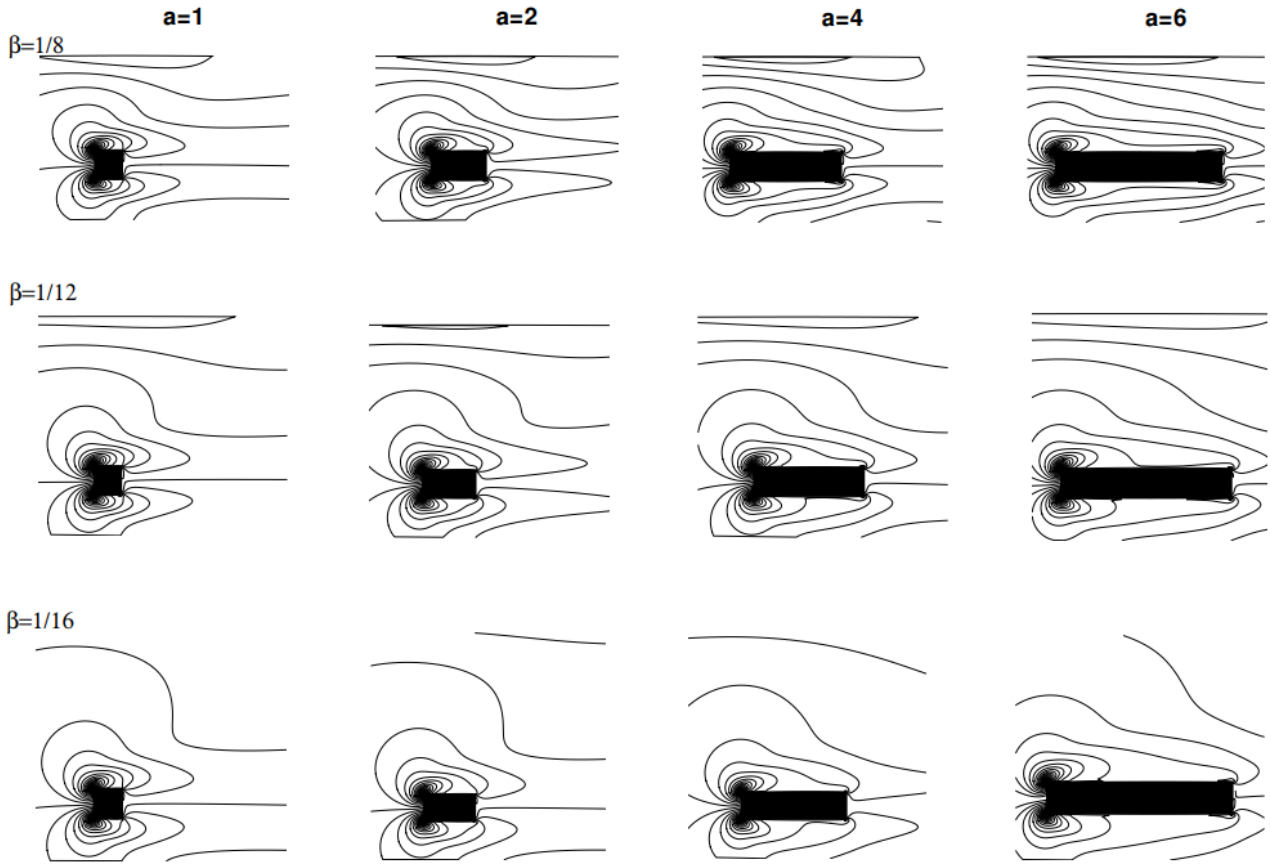

Fig. 4. Vorticity patterns for different aspect ratio of rectangular cylinder (*a* = 1, 2, 3, 4) and blockage ratio (*β* = 1/8, 1/12.1/16) at *Re* = 40

6.3 Drag Phenomenon

The drag force experienced by rectangular cylinder in a cross flow is consist of two components, viz. pressure or form drag coefficient (C_{DP}) and viscous drag coefficient (C_{DF}). The summation of both coefficients comprises the total drag coefficient (C_D). The effect of blockage ratio (β) for different aspect ratio (a_r) of rectangular cylinder is presented in Table 3. As expected, the drag coefficient value for confined cylinder should be more than that of unconfined cylinder. Intuitively, with the increase in blockage ratio, flow behavior shows more and more characteristics of unconfined cylinder flow. The increase in blockage ratio (decrease in wall confinement) causes linear decrease in drag coefficient values. This is due to the fact that the increase in blockage ratio, the flow behavior become equivalent to unconfined flow causing decrease in pressure exerted on cylinder wall as well as viscous

dissipation. For a constant blockage ratio, the drag values vary linearly with aspect ratio of rectangular cylinder. As increase in aspect ratio causes increase in the area of rectangular cylinder, which in turns increases the drag experienced on the rectangular cylinder. So, it can be concluded that the aspect ratio (a_r) of rectangular cylinder and blockage ratio (β) have an opposing effect on drag values, i.e., drag values varies in inverse and proportionally with aspect ratio and blockage ratio, respectively. The values of pressure drag coefficient are always higher than that of viscous drag coefficient. This suggests dominant role of pressure force on square cylinder walls, which is similar with previous studies [15,27]. Thus, the drag coefficient shows complex dependence on blockage ratio and aspect ratio.

Table 3
Drag coefficient results for different values of blockage ratio (β) and aspect ratio of rectangular cylinder (a) at Re = 40

	Re = 40		
Aspect ratio (a)	C_{DP}	C_{DF}	C_D
β = 1/8			
1	1.511	0.271	1.782
2	1.319	0.246	1.565
4	1.619	0.371	1.990
6	1.784	0.518	2.302
β = 1/12			
1	1.319	0.246	1.565
2	1.151	0.181	1.332
4	1.163	0.283	1.446
6	1.183	0.378	1.561
β = 1/16			
1	1.315	0.174	1.101
2	0.960	0.162	1.122
4	0.958	0.247	1.204
6	0.978	0.323	1.300

6.4 Variation of Surface Pressure Coefficient (C_P)

The influence of pressure on the walls of square cylinder with respect to free stream pressure is explained by non-dimensional factor called surface pressure coefficient (C_P) (Eq. (14)). The influence of blockage ratio at Reynolds number of 40 on the surface pressure coefficient along the rectangular cylinder surface of different aspect ratio is shown in Figure 5. As anticipated, higher values of C_P are obtained for front face of cylinder. By reducing the channel confinement, i.e., increasing blockage ratio, decreases the C_P value for fixed Reynolds number. No significant changes are observed in C_P values with aspect ratio along the front and rear surface of rectangular cylinder, as the height of cylinder of varying aspect ratio is same (only width has been changed). Thus, the same level of pressure is exerted on the front and rear surface of cylinder. But significant changes are observed in C_P values along vertical and horizontal surfaces of rectangular cylinder. Thus, the surface pressure coefficient (C_P) varies inversely with blockage ratio and has no substantial effect of aspect ratio of rectangular cylinder.

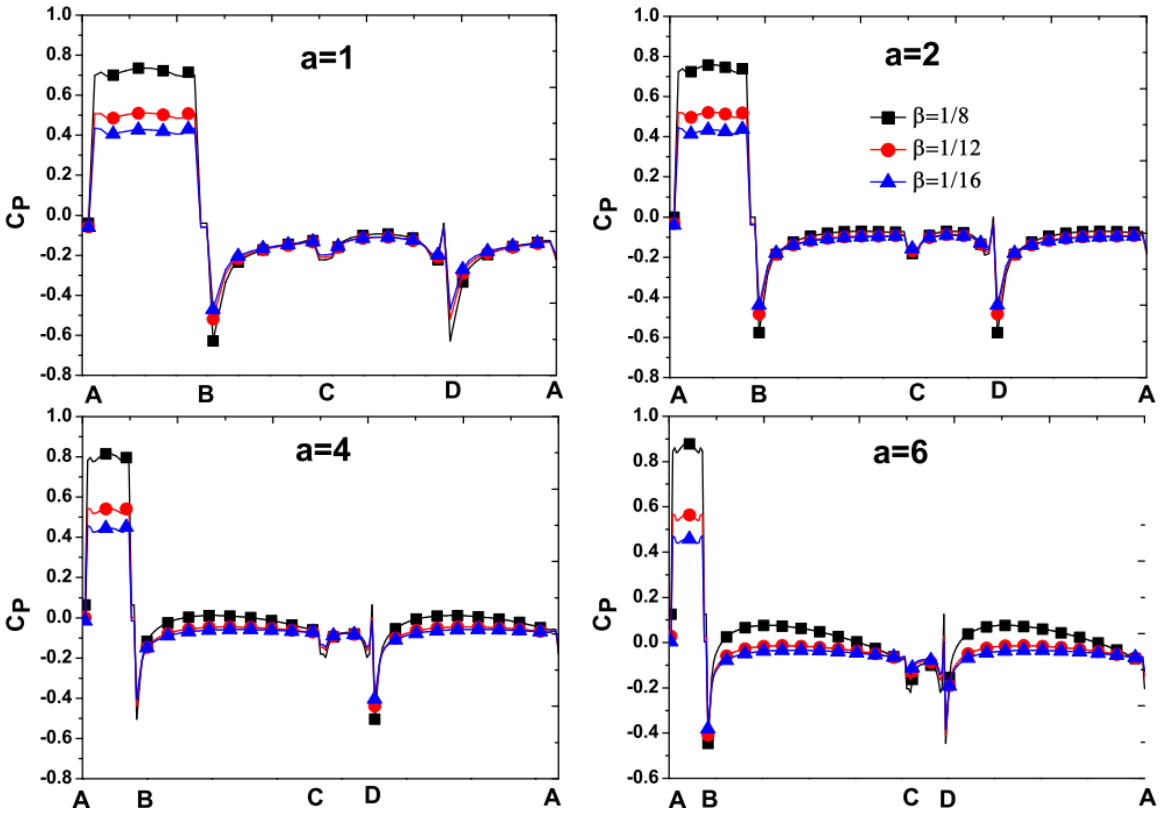

Fig. 5. Pressure coefficient (C_P) variation along surface of square cylinder for different aspect ratio (a = 1, 2, 4, 6) and blockage ratio (β = 1/8, 1/12, 1/16) at Re = 40

6.5 Empirical Correlation

For the scientific and engineering applications, it is worth to develop a simple closure relationship presenting the functional dependencies of gross engineering parameters (drag coefficient, average Nusselt number, etc) on the dimensionless flow governing parameters. It is therefore, considered as an important aspect from an engineering and scientific point of view. The present numerical calculations can be summarized by using an empirical correlation of drag coefficient (C_D). The dependence of drag coefficient on the range of aspect ratio of rectangular cylinder (a_r) and blockage ratio (β) are expressed by using following correlation, which were found to fit the present simulation data satisfactorily:

$$C_D = 7.85\left(\frac{\alpha^{0.122}}{\beta^{0.732}}\right) \qquad \delta_{min} = 0.06\%, \delta_{max} = 3.9\% \tag{31}$$

It can be observed that data fit excellently with R2 values 0.989. Figure 6 presents comparison between drag coefficient C_D obtained from simulation and predicted by Eq. (31).

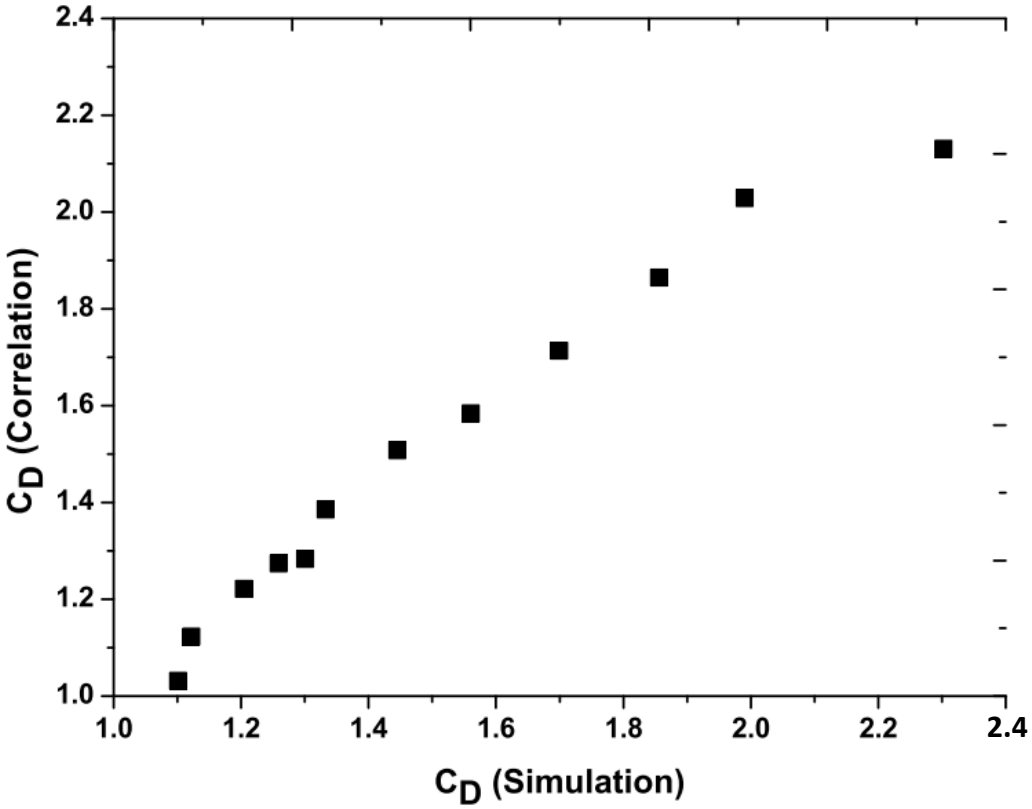

Fig. 6. Comparison of numerical simulation and predicted values of drag coefficient (C_D) (Eq. (31)) for considered range of aspect ratio (a = 1, 2, 4, 6) and blockage ratio (β = 1/8, 1/12, 1/16) at *Re* = 40

7. Conclusions

The numerical study of the laminar steady cross-flow of fluid past a built-in rectangular cylinder by lattice Boltzmann method (LBM) is presented. The effect of blockage ratio ($1/8 \leq \beta \leq 1/20$) and aspect ratio (a_r = 1, 2, 4, 6) on fluid flow characteristics have been elucidated for the Reynolds number of *Re* = 40. The accuracy of present in-house LBM solver (developed in C++ language) is ascertained by grid, domain independence test and validation with literature. The validation of present numerical method with literature shown excellent agreement. The functional dependence of drag coefficient C_D with aspect ratio (a_r) and blockage ratio (β) is obtained by developing simple closure relationship. From this work, following conclusions can be drawn:

(i) The applicability of lattice Boltzmann method for investigating the momentum characteristics of steady cross flow rectangular cylinder in channel is validated by this study.
(ii) The drag values are found to be in inverse proportion with blockage ratio, but varies linearly with aspect ratio of rectangular cylinder.
(iii) The surface pressure coefficient (C_P) varies inversely with blockage ratio and has no substantial effect of aspect ratio of rectangular cylinder. Higher surface pressure coefficient (C_P) values are obtained for front face of cylinder for low blockage ratio.
(iv) Empirical correlations relating total drag coefficient (C_D) with blockage ratio (β) and aspect ratio (a) for *Re* = 40 have been developed for its possible use in engineering design purpose.

References

[1] Chatterjee, Dipankar, Gautam Biswas, and Sakir Amiroudine. "Numerical investigation of forced convection heat transfer in unsteady flow past a row of square cylinders." *International Journal of Heat and Fluid Flow* 30, no. 6

(2009): 1114-1128. https://doi.org/10.1016/j.ijheatfluidflow.2009.09.004
[2] Patil, Pratish P., and Shaligram Tiwari. "Numerical investigation of laminar unsteady wakes behind two inline square cylinders confined in a channel." *Engineering Applications of Computational Fluid Mechanics* 3, no. 3 (2009): 369-385. https://doi.org/10.1080/19942060.2009.11015277
[3] Sharma, Neha, Amit K. Dhiman, and Surendra Kumar. "Mixed convection flow and heat transfer across a square cylinder under the influence of aiding buoyancy at low Reynolds numbers." *International Journal of Heat and Mass Transfer* 55, no. 9-10 (2012): 2601-2614. https://doi.org/10.1016/j.ijheatmasstransfer.2011.12.034
[4] Bharti, Ram Prakash, R. P. Chhabra, and V. Eswaran. "Effect of blockage on heat transfer from a cylinder to power law liquids." *Chemical Engineering Science* 62, no. 17 (2007): 4729-4741. https://doi.org/10.1016/j.ces.2007.06.002
[5] Okajima, Atsushi. "Strouhal numbers of rectangular cylinders." *Journal of Fluid Mechanics* 123 (1982): 379-398. https://doi.org/10.1017/S0022112082003115
[6] Davis, R. W., and E. F. Moore. "A numerical study of vortex shedding from rectangles." *Journal of Fluid Mechanics* 116 (1982): 475-506. https://doi.org/10.1017/S0022112082000561
[7] Davis, R. W., E. F. Moore, and L. P. Purtell. "A numerical-experimental study of confined flow around rectangular cylinders." *The Physics of Fluids* 27, no. 1 (1984): 46-59. https://doi.org/10.1063/1.864486
[8] Norberg, Christoffer. "Flow around rectangular cylinders: pressure forces and wake frequencies." *Journal of Wind Engineering and Industrial Aerodynamics* 49, no. 1-3 (1993): 187-196. https://doi.org/10.1016/0167-6105(93)90014-F
[9] Sohankar, Ahmad, C. Norbergb, and Lars Davidson. "Numerical simulation of unsteady low-Reynolds number flow around rectangular cylinders at incidence." *Journal of Wind Engineering and Industrial Aerodynamics* 69 (1997): 189-201. https://doi.org/10.1016/S0167-6105(97)00154-2
[10] Yang, Suh-Jenq, and Wu-Shung Fu. "Numerical investigation of heat transfer from a heated oscillating rectangular cylinder in a cross flow." *Numerical Heat Transfer Part A-Applications* 39, no. 6 (2001): 569-591. https://doi.org/10.1080/104077801750178879
[11] Nitin, S., and R. P. Chhabra. "Non-isothermal flow of a power law fluid past a rectangular obstacle (of aspect ratio 1×2) in a channel: drag and heat transfer." *International Journal of Engineering Science* 43, no. 8-9 (2005): 707-720. https://doi.org/10.1016/j.ijengsci.2004.12.015
[12] Bruno, Luca, Davide Fransos, Nicolas Coste, and Arianna Bosco. "3D flow around a rectangular cylinder: a computational study." *Journal of Wind Engineering and Industrial Aerodynamics* 98, no. 6-7 (2010): 263-276. https://doi.org/10.1016/j.jweia.2009.10.005
[13] Islam, S. Ul, C. Y. Zhou, A. Shah, and P. Xie. "Numerical simulation of flow past rectangular cylinders with different aspect ratios using the incompressible lattice Boltzmann method." *Journal of Mechanical Science and Technology* 26 (2012): 1027-1041. https://doi.org/10.1007/s12206-012-0328-4
[14] Chen, Ye Jun, and Chuan Ping Shao. "Suppression of vortex shedding from a rectangular cylinder at low Reynolds numbers." *Journal of Fluids and Structures* 43 (2013): 15-27. https://doi.org/10.1016/j.jfluidstructs.2013.08.001
[15] Dhiman, A. K., R. P. Chhabra, and V. Eswaran. "Flow and heat transfer across a confined square cylinder in the steady flow regime: effect of Peclet number." *International Journal of Heat and Mass Transfer* 48, no. 21-22 (2005): 4598-4614. https://doi.org/10.1016/j.ijheatmasstransfer.2005.04.033
[16] Gupta, Abhishek K., Atul Sharma, Rajendra P. Chhabra, and Vinayak Eswaran. "Two-dimensional steady flow of a power-law fluid past a square cylinder in a plane channel: momentum and heat-transfer characteristics." *Industrial & Engineering Chemistry Research* 42, no. 22 (2003): 5674-5686. https://doi.org/10.1021/ie030368f
[17] Chen, Shiyi, and Gary D. Doolen. "Lattice Boltzmann method for fluid flows." *Annual Review of Fluid Mechanics* 30, no. 1 (1998): 329-364. https://doi.org/10.1146/annurev.fluid.30.1.329
[18] Sivakumar, P., Ram Prakash Bharti, and R. P. Chhabra. "Steady flow of power-law fluids across an unconfined elliptical cylinder." *Chemical Engineering Science* 62, no. 6 (2007): 1682-1702. https://doi.org/10.1016/j.ces.2006.11.055
[19] Perumal, D. Arumuga, and Anoop K. Dass. "Simulation of Incompressible Flows in Two-Sided Lid-Driven Square Cavities: Part II-LBM." *CFD Letters* 2, no. 1 (2010): 25-38.
[20] Perumal, D. Arumuga, Gundavarapu V. S. Kumar, and Anoop K. Dass. "Lattice Boltzmann simulation of viscous flow past elliptical cylinder." *CFD Letters* 4, no. 3 (2012): 127-139.
[21] Dong, Yinfeng, Jianying Zhang, and Guangwu Yan. "A higher-order moment method of the lattice Boltzmann model for the conservation law equation." *Applied Mathematical Modelling* 34, no. 2 (2010): 481-494. https://doi.org/10.1016/j.apm.2009.06.024
[22] Xi, Haowen, Gongwen Peng, and So-Hsiang Chou. "Finite-volume lattice Boltzmann method." *Physical Review E* 59, no. 5 (1999): 6202. https://doi.org/10.1103/PhysRevE.59.6202
[23] Zhang, Raoyang, and Hudong Chen. "Lattice Boltzmann method for simulations of liquid-vapor thermal flows." *Physical Review E* 67, no. 6 (2003): 066711. https://doi.org/10.1103/PhysRevE.67.066711

[24] Sukop, Michael C., and Daniel T. Jr Thorne. *Lattice Boltzmann modeling: an introduction for geoscientists and engineers*. Springer, 2007. https://doi.org/10.1007/978-3-540-27982-2
[25] Mohamad, A. A. *Lattice boltzmann method*. Vol. 70. London: Springer, 2011. https://doi.org/10.1007/978-0-85729-455-5
[26] Zou, Qisu, and Xiaoyi He. "On pressure and velocity boundary conditions for the lattice Boltzmann BGK model." *Physics of Fluids* 9, no. 6 (1997): 1591-1598. https://doi.org/10.1063/1.869307
[27] Dhiman, A. K., R. P. Chhabra, and V. Eswaran. "Steady flow across a confined square cylinder: Effects of power-law index and blockage ratio." *Journal of Non-Newtonian Fluid Mechanics* 148, no. 1-3 (2008): 141-150. https://doi.org/10.1016/j.jnnfm.2007.04.010
[28] Bouaziz, Mohamed, Sameh Kessentini, and Saïd Turki. "Numerical prediction of flow and heat transfer of power-law fluids in a plane channel with a built-in heated square cylinder." *International Journal of Heat and Mass Transfer* 53, no. 23-24 (2010): 5420-5429. https://doi.org/10.1016/j.ijheatmasstransfer.2010.07.014
[29] Bharti, Ram Prakash, R. P. Chhabra, and V. Eswaran. "Steady forced convection heat transfer from a heated circular cylinder to power-law fluids." *International Journal of Heat and Mass Transfer* 50, no. 5-6 (2007): 977-990. https://doi.org/10.1016/j.ijheatmasstransfer.2006.08.008